JTCM Journal of Traditional Chinese Medicine

Online Submissions: http://www.journaltcm.com
ISSN 0255-2922
info@journaltcm.com

Original Article

Integration of serum pharmacochemistry with network pharmacology to reveal the potential mechanism of Yangqing Chenfei formula (养清尘肺方) for the treatment of silicosis

HU Yuanyuan, LIU Xinguang, ZHAO Peng, WU Jinyan, YAN Xinhua, HOU Runsu, WANG Xiangcheng, YANG Fan, TIAN Xinrong, LI Jiansheng

HU Yuanyuan, Longhua Hospital Shanghai University of Traditional Chinese Medicine, Shanghai University of Traditional Chinese Medicine, Shanghai 200032, China
LIU Xinguang, ZHAO Peng, WU Jinyan, YAN Xinhua, HOU Runsu, WANG Xiangcheng, YANG Fan, TIAN Xinrong, LI Jiansheng, Co-construction Collaborative Innovation Center for Chinese Medicine and Respiratory Diseases by Henan and Education Ministry of P.R. China. Zhengzhou, 450046, China; Henan Key Laboratory of Chinese Medicine for Respiratory Disease, Henan University of Chinese Medicine, Zhengzhou 450046, China
Supported by Special Project of Traditional Chinese Medicine Research in Henan Province: Evaluation and Characteristics of the Therapeutic Effect of Dialectical Treatment for Coal Worker Pneumoconiosis Based on Multicenter, Randomized, Double-Blind, and Parallel Controlled Trials (No. 20-21ZYZD01)
Correspondence to: LI Jiansheng, Co-construction Collaborative Innovation Center for Chinese Medicine and Respiratory Diseases by Henan and Education Ministry of China, Zhengzhou 450046, China; Henan Key Laboratory of Chinese Medicine for Respiratory Disease, Henan University of Chinese Medicine, Zhengzhou 450046, China. li_js8@163.com
Telephone: +86-371-65676568
DOI: 10.19852/j.cnki.jtcm.20240610.005
Received: November 22, 2022
Accepted: April 28, 2023
Available online: June 10, 2024

Abstract

OBJECTIVE: To explore the mechanisms of Yangqing Chenfei formula (养清尘肺方, YCF) in the treatment of silicosis through a comprehensive strategy consisting of serum pharmacochemistry, network pharmacology analysis, and *in vitro* validation.

METHODS: An ultrahigh-performance liquid chromatography-tandem mass spectrometry method was used to confirm the active components in YCF-medicated serum. Then, we obtained targets for active components and genes for silicosis from multiple databases. Furthermore, a protein-protein interaction network was constructed, and Kyoto Encyclopedia of Genes and Genomes pathway and biological process analyses were conducted to elucidate the mechanisms of YCF for the treatment of silicosis. Finally, we validated the important components and mechanisms *in vitro*.

RESULTS: Altogether, 19 active components were identified from rat serum after YCF administration. We identified 724 targets for 19 components, which were mainly related to inflammation [phosphatidy linositol 3 kinase/protein kinase B, forkhead box O, hypoxia inducible factor, and T-cell receptor signaling pathway, nitric oxide biosynthetic process], fibrotic processes [vascular endothelial growth factor signaling pathway, extracellular signal regulated kinase (ERK) 1 and ERK2 cascade, smooth muscle cell proliferation], and apoptosis (negative regulation of apoptotic process). In addition, 218 genes for silicosis were identified and were mainly associated with the inflammatory response and immune process [cytokine–cytokine receptor interaction, tumor necrosis factor alpha (TNF-α), toll-like receptor, and nucleotide binding oligomerization domain-like receptor signaling pathway]. Taking an intersection of active component targets and silicosis genes, we obtained 61 common genes that were mainly related to the inflammatory response and apoptosis, such as the phosphatidylinositol-3-kinase/protein kinase B signaling pathway, mitogen activated protein kinases signaling pathway, TNF signaling pathway, toll-like receptor signaling pathway, biosynthesis of nitric oxide, and apoptotic process. In the herb-component-gene-pathway network, paeoniflorin, rutin and nobiletin targeted the most genes. *In vitro*, paeoniflorin, rutin and nobiletin decreased the mRNA levels of inflammatory factors [interleukin (IL)-6, TNF-α, and IL-1β], suppressed p-AKT and cleaved caspase-3, and increased B cell lymphoma (Bcl)-2 protein expression in silica-induced macrophages in a concentration-dependent manner.

CONCLUSION: YCF could significantly relieve the inflammatory response of silicosis *via* suppression of the AKT/Bcl-2/Caspase-3 pathway.

Keywords: silicosis; network pharmacology; validation study; serum pharmacochemistry; Yangqing Chenfei formula

1. INTRODUCTION

Silicosis, a widespread and serious occupational lung

disease in the world, is caused by long-term exposure to silica.[1,2] Approximately 230 million people worldwide, mostly from the construction and mining industries, are exposed to silica every year.[3-5] The number of silicotic patients increased by 66.0% from 1990 to 2017.[6] A persistent inflammatory response is the main pathological process of silicosis, which eventually leads to pulmonary fibrosis. Evidence suggests that silica significantly increases the levels of inflammatory cells (macrophages, neutrophils, and lymphocytes) and inflammatory cytokines [tumor necrosis factor alpha (TNF)-α, interleukin (IL)-1β, and IL-6] in the lung tissues and bronchoalveolar lavage fluid of silicosis mice.[7,8] Furthermore, silica could activate the protein kinase B (AKT)/Caspase-3 signaling pathway, initiate macrophage apoptosis, and aggravate the release of inflammatory cytokines, ultimately leading to pulmonary inflammatory injury and fibrosis.[9,10]

To date, there is no effective treatment for silicosis. Traditional Chinese Medicine (TCM) has been proven to be beneficial for silicotic patients. Yangqing Chenfei formula (养清尘肺方, YCF), consisting of Maidong (*Radix Ophiopogonis Japonici*), Xiyangshen (*Radix Panacis Quinquefolii*), Xuanshen (*Radix Scrophulariae*), Gualou (*Fructus et Semen Trichosanthis*), Zhebeimu (*Bulbus Fritillariae Thunbergii*), Chishao (*Radix Paeoniae Rubra*), Yujin (*Radix Curcumae Wenyujin*), Ziwan (*Radix Asteris Tatarici*), Chenpi (*Pericarpium Citri Reticulatae*), Jiegeng (*Radix Platycodi*), is a formula for silicotic patients with yin deficiency and heat dryness syndrome. Multicenter randomized double-blind clinical studies have shown that YCF could effectively relieve the symptoms of cough, expectoration, shortness of breath, and dyspnea, improve the 6-minute walking distance, and reduce the St. George's Respiratory Questionnaire score,[11] but the exact mechanisms need to be further studied.

However, the multicomponent, multitarget and multichannel characteristics of TCM make its therapeutic mechanisms difficult to understand. Network pharmacology provides an effective method to study the mode of action of TCM.[12-14] However, most network pharmacology for TCM prescriptions usually selects components from the TCM database according to oral bioavailability but neglects the influence of other components on oral bioavailability.[15,16] This will result in a deviation from the actually absorbed ingredients. Serum pharmacochemistry of TCMs could analyze and identify the effective components in TCM medicated-serum *via* liquid chromatography, mass spectrometry and other identification methods.[17] Compared with searching the TCM database, using serum pharmacochemistry to identify the active ingredients of TCM prescriptions that are actually present in serum will increase the accuracy of target prediction.

In this study, we explored the active ingredients and molecular functions of YCF for the treatment of silicosis *via* serum pharmacochemistry and network pharmacology. Ultrahigh-performance liquid chromatography-tandem mass spectrometry (UPLC-MS/MS) was used to determine active components from rat serum after oral administration of YCF. Furthermore, we obtained targets for active components and genes for silicosis by searching multiple databases. Then, we constructed a network and performed functional analysis to illustrate the potential mechanisms of YCF in treating silicosis. Finally, cell experiments were conducted to validate the molecular mechanisms predicted by network pharmacology.

2. METHODS AND MATERIALS

2.1. Materials

LC-MS grade acetonitrile, formic acid and high-performance liquid chromatography-grade methanol were purchased from Thermo Fisher Technology Co., Ltd. (Shanghai, China). Standards of arginine, aspartic acid, baicalin, inositol, fusetin, actinoside, hyperoside, harpagoside, nobiletin, esculetin, synephrine, protocatechuic acid, eriocitrin, esculin, gallic acid, ginsenoside Rb1, L-malic acid, narirutin, nobiletin, oxypaeoniflorin, paeoniflorin, paeonol, peiminine, rutin, scopoletin, tangeretin and threonine were purchased from Shanghai Yuanye Technology Co., Ltd. (Shanghai, China).

2.2. Preparation of YCF

All herbs of YCF were provided by Ruilong Pharmaceutical Co., Ltd. (Zhengzhou, China). YCF extract was prepared in fluid extract according to the standard operating procedure. YCF extract (0.2 mg) was mixed with 20 mL 70% methanol, and then the mixture was ultrasonicated and centrifuged. The supernatant was deposited at −20 ℃ for testing.

2.3. Animal experiment

Male Sprague-Dawley rats (n = 20, age = 2 months, 180-200 g) were provided by Beijing Weitong Lihua Experimental Animals Co., Ltd. [No. SCXK (jing) 2016-0006]. All rats were housed in individually ventilated cages (CA25; Fengshi, Suzhou, China) and provided free access to sterile food and water. The environmental temperature was controlled at 20-25 ℃. The animal study was reviewed by the Experimental Animal and Ethics Committee of the First Affiliated Hospital, Henan University of Chinese Medicine.The rats were randomly divided into a control group (n =10, 2 mL/d 0.9% normal saline IG) and a YCF group (n = 10, 48.6 $g \cdot kg^{-1} \cdot d^{-1}$ YCF extract IG). The human equivalent doses of YCF were calculated using Equation 1, where D = dose (mg/kg); K = body shape index; and W = body weight. After corresponding treatment for 7 d, rats were euthanized . Blood samples were harvested 2 h after oral administration *via* the oculi chorioidea vein. Then, the serum samples were separated and stored at −80 ℃ until analysis.

$$D_{rat} = D_{human} \times \left(\frac{K_{rat}}{K_{human}}\right) \times \frac{\left(\frac{W_{rat}}{W_{human}}\right)^2}{3} \quad (1)$$

2.4. Preparation of serum samples

A protein precipitation procedure was used to extract components from medicated serum of YCF. One hundred microliters of serum were mixed with 300 μL of acetonitrile. The mixture was vortex-mixed for 3 min and allowed to stand for 5 min at 4 ℃. After centrifugation at 13 000 rpm for 10 min at 4 ℃, 300 μL of supernatant liquid was collected into a new tube and dried. The dried extract was mixed with 50 μL of 50% acetonitrile, and 35 μL of supernatant was taken for analysis.

2.5. Identification of active components

We combined a Dionex Ultimate 3 000 UPLC system (Thermo Fisher Scientific, Germering, Germany) with a Thermo Scientific Q Exactive Orbitrap mass spectrometer (Thermo Fisher Scientific, Bremen, Germany) for the analysis of the YCF extract and medicated serum.

The samples were added to a Phenomenex Synergi Polar-RP (Los Angeles, CA, USA) (2 mm × 150 mm, 4 μm) at 40 ℃. Mobile phase A was water and 0.1% formic acid. Mobile phase B was ACN and 0.1% formic acid. The gradient elution conditions were as follows: 0% B (0-5 min), 0% B to 22% B (5-14 min), 22% B to 28% B (14-20 min), 28% B to 36% B (20-36 min), 36% B to 45% B (36-42 min), 45% B to 100% B (42-62 min), 100% B (62-67 min), then back to 0% B (67-69 min), and finally stopped at 69 min. The flow rate was 0.3 mL/min, and the sample volume was 5 μL.

The mass spectrometer was equipped with an electrospray ion source, and the spray voltage for positive/negative ion mode was set at 3 500 V/2 800 V. Sheath gas and aux gas were set at 40 and 10 Arb, respectively. The capillary temperature and aux gas heater temperature were set at 325 ℃ and 300 ℃, respectively. Full scans were performed from m/z 100 to 1500 at a resolution of 70 000, an auto gain control (AGC) target of 3×10^6 and a maximum injection time of 0.2 s. The target MS2 scan was performed at a resolution of 17 500 K, the isolation width was set as 4.0 Da, with an AGC target of 2×10^5 and a maximum injection time of 0.1 s.

2.6. Targets and gene prediction

Targets for the active component of YCF were obtained from the Traditional Chinese Medicine systems pharmacology (TCMSP) (https://old.tcmsp-e.com/tcmsp.php), PharmMapper (http: //www.lilab-ecust.cn/pharmmapper/), and SwissTargetPrediction (http: //www.swisstargetprediction.ch/) databases. Genes of silicosis were obtained from the Comparative Toxicogenomics Database (CTD) (http: //ctdbase.org/), DisGeNET (https: //www.disgenet.org/) and GeneCards (https: //www.genecards.org/) databases. Only genes related to silicosis that appeared in 2 or 3 databases were accepted. All protein names were transformed into gene names in the UniProt (https://www.uniprot.org/) database.

2.7. Network construction

Active component targets and silicosis genes were brought into the STRING (https: //cn.string-db.org/) database to obtain the interacting proteins, restricted organism as “Homo sapiens”. Consequently, protein–protein interaction (PPI) networks were constructed using Cytoscape 3.8.2, and subnetworks were extracted according to node degree. The herb-component-target network and herb-component-gene-pathway network were established using Cytoscape 3.8.2.

2.8. Functional enrichment analysis

Kyoto Encyclopedia of Genes and Genomes (KEGG) pathway and biological process (BP) enrichment analyses were performed by Database for Annotation, Visualization and Integrated Discovery (DAVID) (https: //david.ncifcrf.gov/). All results were visualized by Bioinformatics (http: //www.bioinformatics.com.cn/).

2.9. Cell culture and treatment

Mouse alveolar macrophages (MHS) were purchased from Zishi Biological Technology Co., Ltd. (20210406-2114Y, Shanghai, China) and maintained in 1640 medium (Solarbio, 31 800, Beijing, China) supplemented with 4.5 g/L glucose, 100 U/mL penicillin, 100 μg/mL streptomycin and 10% fetal bovine serum (Lonsera, Montevideo, Uruguay) in a humidified atmosphere containing 5% CO_2 at 37 ℃.

The MHS cells were plated into 96-well plates (1.0×10^4 cells/well). Then, the cells were treated with different concentrations of active components for 6 h. Next, the medium was replaced with 100 μL of 1 640 medium containing 10 μL of CCK8 reagent (Abbkine, KTA1 020, Wuhan, China). After 1 h of culture, the absorbance of each well was recorded at 450 nm by a microplate reader Thermo, Waltham, MA, USA).

The MHS cells were plated into 6-well plates (1.0×10^6 cells per well). Cells were treated with different concentrations of active components and stimulated simultaneously with silica (50 μg/cm^2) for 6 h. The cells were collected for further analysis.

2.10. Western blot assay

Total protein of MHS cells was extracted by using icedradio immunoprecipitation assay buffer. The protein concentration was determined by bicinchoninic acid assay. Equal amounts of protein were fractionated by electrophoresis on 12.5% sodium dodecyl sulfate-polyacrylamide gel electrophoresis gels and then transferred to polyvinylidene difluoride (PVDF) membranes (Millipore, Boston, MA, USA). The membranes were blocked with 5% (w/v) nonfat milk and then incubated with primary antibodies [anti-AKT (1∶1000 dilution, 4685S, CST, Beverly, MA, USA), anti-p-AKT (1∶1000 dilution, 4060S, CST, Beverly, MA, USA), anti-Bcl-2 (1∶1000 dilution, 12789-T-AP, Proteintech, Wuhan, China), anti-cleaved caspase-3 (1∶1000 dilution, 9664, CST, Beverly, MA, USA), and anti-glyceraldehyde-3-phosphate dehydrogenase (1∶5000 dilution, 10494-1-AP, Proteintech, Wuhan, China)] at 4 ℃ overnight. Subsequently, the PVDF

membranes were washed and incubated with secondary antibodies at room temperature for 1 h. Finally, the bands were visualized by an enhanced chemiluminescence kit (yamei, Shanghai, China) and imaging system (ChemiDoc MP, Hercules, CA, USA), and quantified by Image Lab software.

2.11. Real-time quantitative polymerase chain reaction (qPCR) assay

Total RNA was extracted using QIAzol lysis reagent (Qiagen, 79306, Dusseldorf, Germany) following the manufacturer's instructions and reverse-transcribed into cDNA with the HiScript®IIQ RT SuperMix kit (Vazyme, R223, Nanjing, China). Then, the cDNA was used for qPCR with the ChamQ Universal Synergy Brands qPCR Master Mix kit (Vazyme, Q711, Nanjing, China). Mubb was used as an internal control. The sequences of the primer pairs were IL-6 F: CTGCAAGAGACTTCCA-TCCAG, IL-6 R: AGTGGTATAGACAGGTCTGTTGG; IL-1β F: GAAATGCCACCTTTTGACAGTG, IL-1β R: TGGATGCTCTCATCAGGACAG; TNF-α F: CAGG-CGGTGCCTATGTCTC, TNF-α R: CGATCACCCCG-AAGTTCAGTAG; Mubb F: TGGCTATTAATTATT-CGGTCTGCA, Mubb R: GCAAGTGGCTAGAGTG-CAGAGTAA.

2.12. Statistical analysis

The data were analyzed using SPSS statistics 22.0 software (IBM Corp., Armonk, NY, USA) and expressed as the mean ± standard deviation. One-way analysis of variance was performed to detect significant differences among the groups. $P < 0.05$ was considered significant.

3. RESULTS

3.1. Chemical profiling of components in the YCF extract

A UPLC-Q-MS/MS method was used to identify chemical constituents in the YCF extract *via* positive and negative modes. As shown in supplementary Figure 1A, 270 chemical constituents were identified from the YCF extract according to the MS information, fragmentation pattern of standards and published reports. Among the 270 chemical constituents, 14 were unique to Zhebeimu (*Bulbus Fritillariae Thunbergii*), 22 to Ziwan (*Radix Asteris Tatarici*), 37 to Chenpi (*Pericarpium Citri Reticulatae*), 29 to Chishao (*Radix Paeoniae Rubra*), 10 to Gualou (*Fructus et Semen Trichosanthis*), 48 to Jiegeng (*Radix Platycodi*), 9 to Maidong (*Radix Ophiopogonis Japonici*), 35 to Xiyangshen (*Radix Panacis Quinquefolii*), 9 to Xuanshen (*Radix Scrophulariae*), 14 to Yujin (*Radix Curcumae Wenyujin*), and 27 compounds were multiple resourced. In addition, the remaining 11 constituents were identified as isomers, and their structures need to be further confirmed. In terms of chemical structure, 61 flavonoids, 61 saponins, 37 saccharides, 24 alkaloids, 17 organic acids, 12 fatty acids, 10 terpenoids, 7 coumarins, 6 amino acids, and 35 other compounds were identified from the YCF extract. According to the retention time and MS spectra of standards, 28 chemical ingre

3.2. Chemical profiling of YCF-medicated serum

We further conducted chemical profiling of ingredients in YCF-medicated serum. In total, 128 prototype components were determined in YCF-medicated serum, including 29 saponins, 24 flavonoids, 17 alkaloids, 16 saccharides, 12 organic acids, 6 amino acids, 5 coumarins, 4 fatty acids, 1 terpenoid, and 14 other compounds. After comparison with the standards, 19 components were identified from YCF-medicated serum (Table 1, supplementary Figure 1B).

3.3. Functional analysis of the candidate active component targets

The 19 components identified from YCF-medicated serum may exert a comprehensive effect by acting on

Table 1 Information of the 19 active components in YCF medicated-serum

No.	Component	Formula	RT	m/z
1	Arginine	$C_6H_{14}N_4O_2$	1.28	175.12
2	Aspartic acid	$C_4H_7NO_4$	1.32	134.04
3	Baicalin	$C_{21}H_{18}O_{11}$	21.71	447.09
4	Eriocitrin	$C_{27}H_{32}O_{15}$	16.98	595.17
5	Esculin	$C_{15}H_{16}O_9$	13.39	339.07
6	Gallic acid	$C_7H_6O_5$	4.17	169.01
7	Ginsenoside Rb1	$C_{54}H_{92}O_{23}$	26.34	1109.61
8	L-Malic acid	$C_4H_6O_5$	1.64	133.01
9	Narirutin	$C_{27}H_{32}O_{14}$	18.53	581.19
10	Nobiletin	$C_{21}H_{22}O_8$	39.61	403.14
11	Oxypaeoniflorin	$C_{23}H_{28}O_{12}$	13.97	495.15
12	Paeoniflorin	$C_{23}H_{28}O_{11}$	15.83	479.16
13	Paeonol	$C_9H_{10}O_3$	28.07	167.07
14	Peimine	$C_{27}H_{45}NO_3$	20.61	432.35
15	Peiminine	$C_{27}H_{43}NO_3$	22.09	430.33
16	Rutin	$C_{27}H_{30}O_{16}$	16.88	609.15
17	Scopoletin	$C_{10}H_8O_4$	18.34	193.05
18	Tangeretin	$C_{20}H_{20}O_7$	43.03	373.13
19	Threonine	$C_4H_9NO_3$	1.32	120.07

Notes: YCF: Yangqing Chenfei formula.

multiple targets. We obtained 724 targets for the 19 active components from the TCMSP, PharmMapper, and SwissTargetPrediction databases and then constructed an herb-component-target network (750 nodes, 5 626 edges, supplementary Figure 1C). In the network, tangeretin connected the most targets, followed by rutin and esculin. To better analyze the effect of targets, top 100 hub targets (supplementary Figure 2B) were screened out from the PPI network of 724 active component targets according to their degree value, and KEGG and BP analyses were performed. Subsequently, 125 KEGG terms and 543 biological process terms were enriched with the top 100 hub targets. The top 20 KEGG pathways (Figure 1A) and top 10 biological processes (Figure 1B) could be categorized as inflammation regulation [forkhead box protein O (FoxO) signaling pathway, hypoxia inducible factor (HIF)-1 signaling pathway, phosphatidy linositol 3 kinase/protein kinase B (PI3k-AKT) signaling pathway, nitric oxide biosynthetic process], immune reaction (hepatitis B, influenza A, T-cell receptor signaling pathway), fibrotic process [vascular endothelial growth factor (VEGF) signaling pathway, focal adhesion, cell proliferation, ERK1 and ERK2 cascade, smooth muscle cell proliferation], cell apoptosis (apoptotic process), and so on. In addition, the top 20 targets (supplementary Figure 2C) were mainly associated with inflammation [IL6, TNF, IL1B, latrix metalloproteinase (MMP) 9, AKT1, and signal transducer and activator of transcription (STAT) 3], fibrotic processes [vascular endothelial growth factor A and epidermal growth factor receptor], and apoptosis [cysteinyl aspartate specific proteinase (CASP) 3]. Therefore, our results indicated that YCF exerts broad therapeutic effects on inflammation, the immune system, fibrosis and apoptosis.

3.4. Functional analysis of silicosis genes

We identified 218 genes for silicosis from the CTD, DisGeNET and GeneCards databases and constructed a PPI network-using Cytoscape. After calculating the degree value, the top 20 genes (supplementary Figure 3C), such as IL6, TNF, IL1B, CXC motif chemokine ligand (CXCL) 8, CC motif Chemokine ligand (CCL) 2, IL4, and toll like receptor (TLR) 4, were mostly related to inflammation. The top 100 genes (supplementary

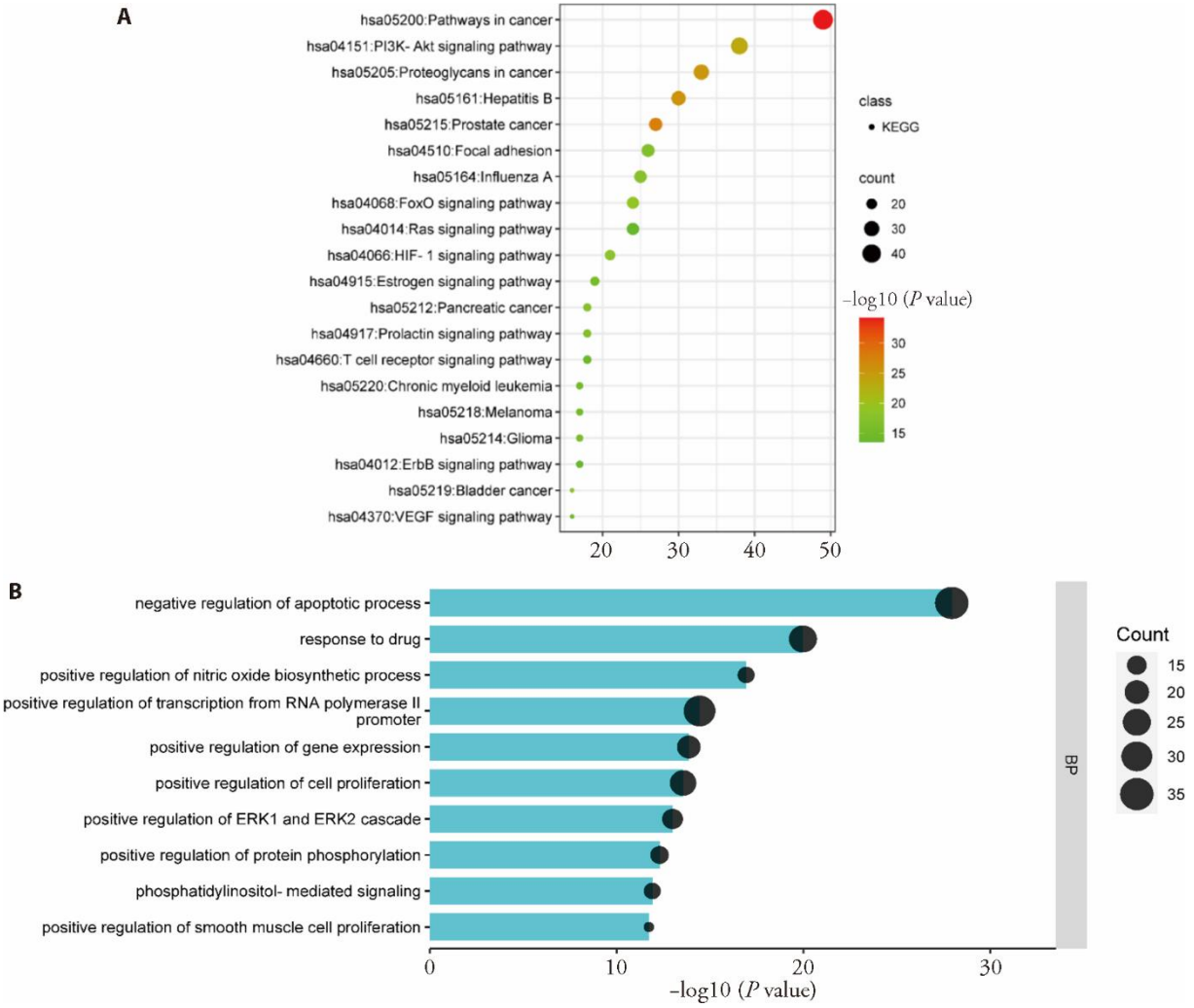

Figure 1 Functional analysis of the active component targets

A: top 20 pathways enriched by the top 100 active component targets; B: top 10 biological processes enriched by the top 100 active component targets. The larger the pvalue, the redder the color. The size of the node is proportional to its count. KEGG: Kyoto Encyclopedia of Genes and Genomes.

Figure 3B) were used to perform KEGG and BP analysis by DAVID, and 109 KEGG terms and 626 BP termswere enriched. In order of *P* values, the top 20 pathways (Figure 2A) and top 10 biological processes (Figure 2B) were mostly associated with inflammation and the immune system, such as the TNF signaling pathway, nucleotide binding oligomerization domain (NOD)-like receptor signaling pathway, toll-like receptor signaling pathway, cellular response to lipopolysaccharide, and cytokine–cytokine receptor interaction. Obviously, the inflammatory reaction was the main pathological mechanism of silicosis.

3.5. Functional analysis of intersecting genes

Taking the intersection of active component targets and silicosis genes, 61 common genes were obtained and used to construct a PPI network (supplementary Figure 4). In order of degree value, the top 10 hub targets, including inflammatory mediators (IL6, TNF, IL1B, MMP9), apoptosis gene (CASP3) and key signaling protein gene (AKT1), were screened out from the PPI network of 61 common genes. Additionally, 100 KEGG terms and 407 BP terms were enriched with the 61 common genes. According to the *P* value, the top 20 pathways (Figure 3A) were related to inflammatory responses, such as the TNF signaling pathway, toll-like receptor signaling pathway, phosphatidylinositol-3-kinase (PI3K)/protein kinase B (AKT) signaling pathway, and mitogen activated protein kinases (MAPK) signaling pathway. As shown in Figure 3B, among the top 5 biological processes, the regulation of the apoptotic process had the highest number of genes. Therefore, we predicted that YCF alleviates the inflammatory response of silicosis *via* regulation of apoptosis. We also constructed an herb-component-target-pathway network, which consisted of 7 herbs, 19 active components, 42 common genes, and the top 20 pathways (88 nodes, 618 edges, Figure 3A). In the network, paeoniflorin, nobiletin and rutin targeted 24, 23 and 22 genes, respectively. These three components may play an important role in the treatment of silicosis. Subsequently, we verified the effects of paeoniflorin, rutin and nobiletin on the inflammatory response in silica-induced macrophages.

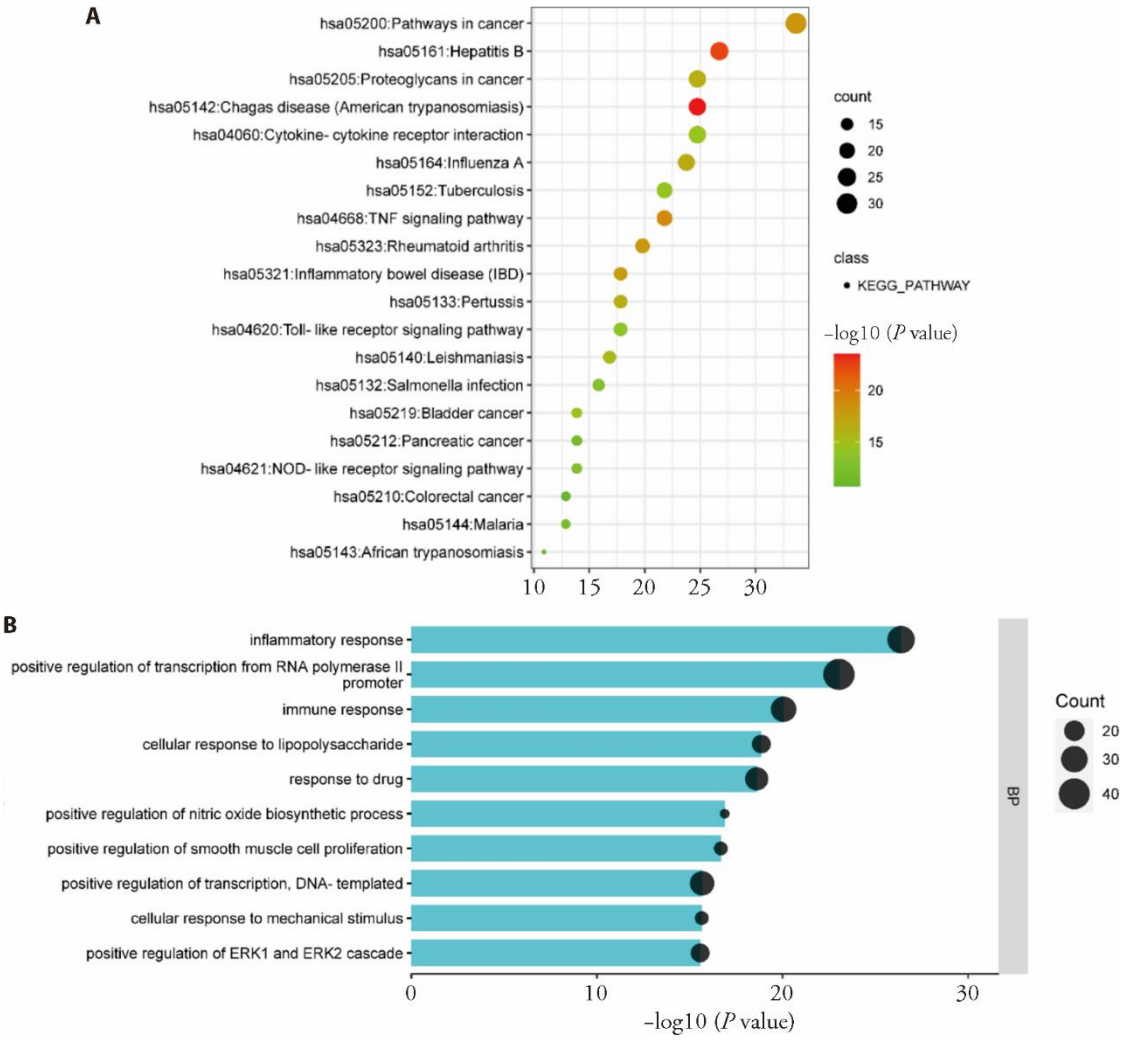

Figure 2 Functional analysis of the silicosis genes

A: top 20 pathways enriched by the top 100 silicosis genes; B: top 10 biological processes enriched by the top 100 silicosis genes. The larger the pvalue, the redder the color. The size of the node is proportional to its count. KEGG: Kyoto Encyclopedia of Genes and Genomes.

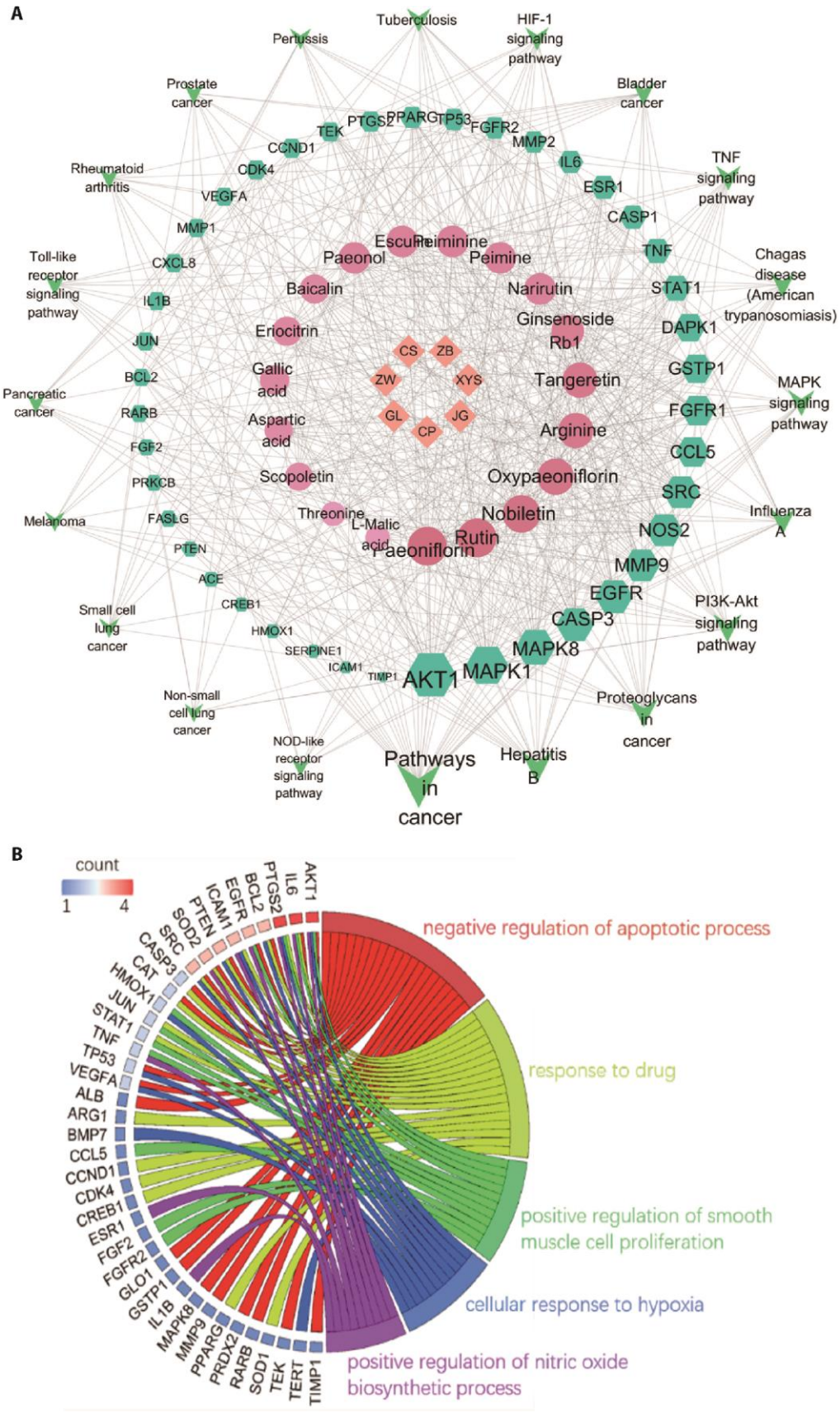

Figure 3 Intersection analysis of active component targets and silicosis genes

A: herb-component-gene-pathway network; B: biological process analysis of 61 common genes. Rhombus represents herb, round represents active component, hexagon represents gene, arrow represents pathway. The size of the node is proportional to its degree. YCF: Yangqing Chenfei formula; ZW: Ziwan (*Radix Asteris Tatarici*); JG: Jiegeng (*Radix Platycodi*); GL: Gualou (*Fructus et Semen Trichosanthis*); ZB: Zhebeimu (*Bulbus Fritillariae Thunbergii*); XYS: Xiyangshen (*Radix Panacis Quinquefolii*); CS: Chishao (*Radix Paeoniae Rubra*); CP: Chenpi (*Pericarpium Citri Reticulatae*).

3.6. YCF inhibits the inflammatory response of silica-induced macrophages

Inflammation is the major characteristic of silicosis, and macrophages are the predominant contributors.[18] Based on the network pharmacology results, both silicosis genes and active component targets were mainly associated with inflammation. Therefore, we detected the effect of paeoniflorin, nobiletin and rutin on the inflammatory response in silica-induced macrophages. As shown in supplementary Figure 5, silica exposure markedly increased the mRNA levels of IL-6, TNF-α and IL-1β in macrophages. However, paeoniflorin, rutin and nobiletin reversed this change in a dose-dependent manner and had no significant effect on cell viability. Therefore, YCF could markedly inhibit the inflammatory response.

3.7. YCF inhibits the AKT/Bcl-2/Caspase-3 pathway in silica-induced macrophages

Given that the PI3K/AKT pathway and apoptosis process are involved in anti-silicosis action, we next used western blotting to determine the effect of active components on the PI3K/AKT pathway and proapoptotic markers. As shown in supplementary Figure 6, silica markedly increased p-AKT and cleaved caspase-3 but decreased Bcl-2 protein expression. In contrast, paeoniflorin, nobiletin and rutin inhibited p-AKT and cleaved caspase-3 protein expression but increased Bcl-2 protein expression in a dose-dependent manner. Consequently, YCF may exert anti-inflammatory effects *via* suppression of the AKT/Bcl-2/Caspase-3 signaling pathways.

4. DISCUSSION

Silicosis is a serious occupational lung disease characterized by chronic inflammation and pulmonary fibrosis, and effective curative medications are still lacking. Emerging evidence indicates the superiority of TCM in treating silicosis.[14,19] YCF, a TCM formula for the treatment of pneumoconiosis, has satisfactory clinical efficacy.[11] *In vivo* studies showed that YCF could remarkably improve the lung function and pathological damage of silicotic rats, reduce the aggregation of fibrocytes and deposition of ECM, and inhibit the infiltration of inflammatory cells and the secretion of inflammatory factors in the lung.[20,21] However, it is difficult to use traditional pharmacological research to identify the effective components and mechanisms of YCF in the treatment of silicosis. Thus, new methods to determine the active components and uncover the mechanisms of YCF for the treatment of silicosis are urgently needed. Herein, a comprehensive strategy consisting of the identification of effective components, functional analysis and validation experiments was used to explore the active components and molecular mechanisms of YCF in treating silicosis.

In this study, 19 active components, such as tangeretin, rutin, esculin, paeoniflorin, and ginsenoside Rb1, were identified from YCF-medicated serum *via* UPLC-MS/MS. These active components, as therapeutic substances of YCF, generally exert multiple bioactivities by acting on multiple proteins. Thus, we identified 724 putative targets for the 19 components. Tangeretin targets the highest number of proteins. The KEGG pathway and biological process analysis indicated that the major bioactivity of targets included the regulation of inflammation, immune response, fibrotic process, and cell apoptosis. Previous research has found that Tangeretin can ameliorate the inflammatory response induced by LPS or IL-1β by inhibiting Notch signaling and PI3K/AKT signaling.[22] Baicalin not only ameliorates neuroinflammation through inhibition of the PI3K/AKT/FoxO1 pathway but also relieves cardiomyocyte apoptosis induced by hypoxia *via* HIF1α/BCL2 interacting protein 3.[23,24] Paeoniflorin exerts anti-inflammatory, antifibrotic and immunomodulatory effects by regulating the MAPK/nuclear factor-kappa, PI3K/AKT, and janus kinase/STAT signaling pathways.[25,26] Rutin and ginsenoside Rb1 have an advantage in reducing proinflammatory markers (IL-6, TNF-α, IL-1β) and proapoptotic markers (Bax, Bcl-2, Caspase-3),[27-31] and ginsenoside Rb1 also has a certain effect on organ fibrosis.[32,33] Furthermore, the 20 hub targets, such as IL6, TNF, IL1B, MMP9, AKT1, and STAT3, were closely related to the inflammatory response. Thus, we can conclude that YCF exerts anti-inflammatory, antifibrotic and antiapoptotic effects *via* regulation of multiple pathways and targets, and the regulation of inflammation is more prominent.

Inflammation is essential for the progression of silicosis and leads to pulmonary fibrosis. The pathways and biological processes enriched by silicosis genes were key signaling pathways in the regulation of inflammation. Furthermore, most of the hub genes, such as CCL2, IL4, CXCL8, IL6, MAPK3, IL10, TLR4, TNF, IL1B, and AKT1, were also closely related to inflammatory and immune responses. For instance, the levels of TNF-α, IL-6 and IL-1β were markedly elevated in the alveolar lavage fluid of silicosis mice.[9] Silica exposure activated the NOD signaling pathway in macrophage cells and initiated the inflammatory response and cell apoptosis.[10] Furthermore, activation of the TLR4/ myeloid differentiation factor 88/TIR domain-containing adaptor protein pathway and NOD-like receptor family protein 3 inflammasome also contributed to the inflammatory response of silicosis.[34,35] These results confirmed that inflammation was the main pathological mechanism in the development of silicosis.

A previous study found that YCF could inhibit the infiltration of inflammatory cells in the lungs of silicotic rats and reduce the release of inflammatory factors.[21] Intersection analysis also suggested that inhibition of inflammation may be the critical mechanism of YCF in treating silicosis. For instance, the top 20 pathways enriched by common genes were important pathways for the regulation of the inflammatory response; hub genes,

such as IL-6, TNF-α, IL-1β, AKT, and MMP9, were closely related to inflammation. Furthermore, the biological process analysis revealed that inhibition of apoptosis may be the underlying mechanism of YCF in alleviating silicotic inflammation. Increasing evidence has shown that apoptosis is closely related to inflammation.[36] We also constructed an herb-component-gene-pathway network. In the network, paeoniflorin targeted the highest number of genes, followed by rutin and nobiletin. These components may play a critical role in the treatment of silicosis. Paeoniflorin has been proven to lower the level of inflammatory cytokines and inhibit cell death by decreasing caspase-3 activity and increasing the Bcl-2/Bax ratio.[37,38] Rutin could lower the levels of TNF-α, IL-6 and IL-1β by suppressing the PI3k-AKT signaling pathway.[30] Nobiletin can also exert protective effects on many diseases *via* suppression of inflammation and apoptosis.[39] Therefore, we predicted that active components of YCF may exert anti-inflammatory effects *via* inhibition of proapoptotic markers for the treatment of silicosis.

Increasing evidence has shown that inflammation is an important pathological process in silicosis and is associated with activation of the AKT/Bcl-2/Caspase-3 pathway.[40] TCM formulas and components have a relatively satisfactory anti-inflammatory effect on silicosis *via* suppression of the AKT-related pathway and apoptosis. Oleanolic acid could decrease the serum level of TNF-α by reducing p-AKT expression in silicotic mice.[41] Coelonin effectively decreased IL-1β, IL-6 and TNF-α mRNA and protein expression, and the inhibition of AKT phosphorylation may be the possible mechanism.[42] Dahuang Zhechong pills (大黄蛰虫丸) reduced the secretion of inflammatory factors in silica-induced MH-S cells by reducing apoptosis.[14] Tre alleviated silica-induced pulmonary inflammation *via* upregulation of Bcl-2 and downregulation of caspase-3.[43] Similarly, our results highlight that paeoniflorin, rutin and nobiletin reduced the mRNA expression of TNF-α, IL-1β and IL-6 and suppressed the AKT/Bcl-2/Caspase-3 pathway in silica-induced macrophages in a concentration-dependent manner. Based on the above results, we predicted that YCF could play an anti-inflammatory role in treating silicosis, and inhibition of the AKT/Bcl-2/Caspase-3 pathway may be the underlying mechanism.

In conclusion, this work uncovered the effective components and pharmacological mechanism of YCF in the treatment of silicosis by using a comprehensive strategy consisting of the identification of effective components, functional analysis and validation experiments. YCF exhibits anti-inflammatory effects *via* suppression of the AKT/Bcl-2/Caspase-3 pathway in treating silicosis.

5. SUPPORTING INFORMATION

Supporting data to this article can be found online at http://journaltcm.cn.

6. REFERENCES

1. Li C, Lu YP, Du ST, et al. Dioscin exerts protective effects against crystalline silica-induced pulmonary fibrosis in mice. Theranostics 2017; 7: 4255-75.
2. Zhou ZW, Jiang R, Yang XY, et al. circRNA mediates silica-induced macrophage activation *via* HECTD1/ZC3H12A-dependent ubiquitination. Theranostics 2018; 8: 575-92.
3. Gottesfeld P, Reid M, Goosby E. Preventing tuberculosis among high-risk workers. Lancet Glob Health 2018; 6: e1274-5.
4. Leung CC, Yu ITS, Chen W. Silicosis. Lancet 2012; 379: 2008-18.
5. Anderson SE, Shane H, Long C, et al. Biological effects of inhaled hydraulic fracturing sand dust. VIII. Immunotoxicity. Toxicol Appl Pharmacol 2020; 408: 115256.
6. Shi P, Xing XY, Xi SH, et al. Trends in global, regional and national incidence of pneumoconiosis caused by different aetiologies: an analysis from the global burden of disease study 2017. Occup Environ Med 2020; 77: 407-14.
7. Santana PT, Luna-Gomes T, Rangel-Ferreira MV, et al. P2Y12 Receptor antagonist clopidogrel attenuates lung inflammation triggered by silica particles. Front Pharmacol 2020; 11: 301.
8. Cao ZJ, Liu Y, Zhang Z, et al. Pirfenidone ameliorates silica-induced lung inflammation and fibrosis in mice by inhibiting the secretion of interleukin-17A. Acta Pharmacol Sin 2022; 43: 908-18.
9. Fan MM, Xiao HJ, Song DY, et al. A novel N-arylpyridone compound alleviates the inflammatory and fibrotic reaction of silicosis by inhibiting the ASK1-p38 pathway and regulating macrophage polarization. Front Pharmacol 2022; 13: 848435.
10. Fu R, Li Q, Fan R, et al. iTRAQ-based secretome reveals that SiO_2 induces the polarization of RAW264.7 macrophages by activation of the NOD-RIP2-NF-κB signaling pathway. Environ Toxicol Pharmacol 2018; 63: 92-102.
11. Li JS, Zhao HL, Xie Y, et al. Clinical efficacy of comprehensive therapy based on Traditional Chinese Medicine patterns on patients with pneumoconiosis: a pilot double-blind, randomized, and placebo-controlled study. Front Med 2022; 16: 736-44.
12. Luo TT, Lu Y, Yan SK, Xiao X, Rong XL, Guo J. Network pharmacology in research of Chinese medicine formula: methodology, application and prospective. Chin J Integr Med 2020; 26: 72-80.
13. Li HY, Zhao LH, Zhang B, et al. A network pharmacology approach to determine active compounds and action mechanisms of ge-gen-qin-lian decoction for treatment of type 2 diabetes. Evid Based Complement Alternat Med 2014; 2014: 495840.
14. Wu LJ, He XY, Wang WX, et al. Dahuang zhechong pills suppress silicosis fibrosis progression *via* p38 MAPK/TGF-β1/Smad pathway *in vitro*. Evid Based Complement Alternat Med 2021; 2021: 6662261.
15. Li MY , Ni J , Yin XB. Research progress on oral bioavailability of traditional chinese medicine preparation. Zhong Hua Zhong Yi Yao Xue Can 2016; 34: 307-11.
16. Yin YH, Zhang K, Wei LY, et al. The molecular mechanism of antioxidation of huolisu oral liquid based on serum analysis and network analysis. Front Pharmacol 2021; 12: 710976.
17. Wang XJ. Studies on serum pharmacochemistry of Traditional Chinese Medicine. Shi Jie Ke Xue Ji Shu-Zhong Yi Yao Xian Dai Hua 2002; 42: 1-4+78.
18. Vanhée D, Gosset P, Boitelle A, Wallaert B, Tonnel AB. Cytokines and cytokine network in silicosis and coal workers' pneumoconiosis. Eur Respir J 1995; 8: 834-42.
19. Liu XY, Wang J, Dou PY, et al. The ameliorative effects of arctiin and arctigenin on the oxidative injury of lung induced by silica *via* TLR-4/NLRP3/TGF-β signaling pathway. Oxid Med Cell Longev 2021; 2021: 5598980.
20. Yang F, Hou RS, Liu XG, et al. Yangqing Chenfei formula attenuates silica-induced pulmonary fibrosis by suppressing activation of fibroblast *via* regulating PI3K/AKT, JAK/STAT, and Wnt signaling pathway. Phytomedicine 2023; 110: 154622.
21. Yan XH. Yangqing chenfei prescription alleviates inflammation

in rat with silicosis *via* NLRP3/Caspase-1 signaling pathway. Henan: Henan University of Chinese Medicine, 2022: 22-6.
22. Li MQ, Zhao Y, Qi D, He J, Wang DX. Tangeretin attenuates lipopolysaccharide-induced acute lung injury through Notch signaling pathway *via* suppressing Th17 cell response in mice. Microb Pathog 2020; 138: 103826.
23. Guo LT, Wang SQ, Su J, et al. Baicalin ameliorates neuroinflammation-induced depressive-like behavior through inhibition of toll-like receptor 4 expression *via* the PI3K/AKT/FoxO1 pathway. J Neuroinflammation 2019; 16: 95.
24. Yu HL, Chen B, Ren Q. Baicalin relieves hypoxia-aroused H9c2 cell apoptosis by activating Nrf2/HO-1-mediated HIF1α/BNIP3 pathway. Artif Cells Nanomed Biotechnol 2019; 47: 3657-63.
25. Zhang LL, Wei W. Anti-inflammatory and immunoregulatory effects of paeoniflorin and total glucosides of paeony. Pharmacol Ther 2020; 207: 107452.
26. Liu X, Chen K, Zhuang YX, et al. Paeoniflorin improves pressure overload-induced cardiac remodeling by modulating the MAPK signaling pathway in spontaneously hypertensive rats. Biomed Pharmacother 2019; 111: 695-704.
27. Tian CL, Shao Y, Jin ZD, et al. The protective effect of rutin against lipopolysaccharide induced acute lung injury in mice based on the pharmacokinetic and pharmacodynamic combination model. J Pharm Biomed Anal 2022; 209: 114480.
28. Arjumand W, Seth A, Sultana S. Rutin attenuates cisplatin induced renal inflammation and apoptosis by reducing NF-κB, TNF-α and caspase-3 expression in wistar rats. Food Chem Toxicol 2011; 49: 2013-21.
29. Muvhulawa N, Dludla PV, Ziqubu K, et al. Rutin ameliorates inflammation and improves metabolic function: a comprehensive analysis of scientific literature. Pharmacol Res 2022; 178: 106163.
30. Sharma A, Tirpude NV, Kumari M, Padwad Y. Rutin prevents inflammation-associated colon damage *via* inhibiting the p38/MAPKAPK2 and PI3K/Akt/GSK3β/NF-κB signalling axes and enhancing splenic Tregs in DSS-induced murine chronic colitis. Food Funct 2021; 12: 8492-506.
31. Rajput SA, Shaukat A, Rajput IR, et al. Ginsenoside Rb1 prevents deoxynivalenol-induced immune injury *via* alleviating oxidative stress and apoptosis in mice. Ecotoxicol Environ Saf 2021; 220: 112333.
32. Hou YL, Tsai YH, Lin YH, Chao JC. Ginseng extract and ginsenoside Rb1 attenuate carbon tetrachloride-induced liver fibrosis in rats. BMC Complement Altern Med 2014; 14: 415.
33. Liu XH, Chen JW, Sun N, et al. Ginsenoside Rb1 ameliorates autophagy *via* the AMPK/mTOR pathway in renal tubular epithelial cells *in vitro* and *in vivo*. Int J Biol Macromol 2020; 163: 996-1009.
34. Chan JYW, Tsui JCC, Law PTW, et al. Regulation of TLR4 in silica-induced inflammation: an underlying mechanism of silicosis. Int J Med Sci 2018; 15: 986-91.
35. Chen SY, Han B, Geng X, et al. Microcrystalline silica particles induce inflammatory response *via* pyroptosis in primary human respiratory epithelial cells. Environ Toxicol 2022; 37: 385-400.
36. Li L, Wan GW, Han B, Zhang ZW. Echinacoside alleviated LPS-induced cell apoptosis and inflammation in rat intestine epithelial cells by inhibiting the mTOR/STAT3 pathway. Biomed Pharmacother 2018; 104: 622-8.
37. Gu XY, Cai ZX, Cai M, et al. Protective effect of paeoniflorin on inflammation and apoptosis in the cerebral cortex of a transgenic mouse model of Alzheimer's disease. Mol Med Rep 2016; 13: 2247-52.
38. Tao YE, Wen ZH, Song YQ, Wang H. Paeoniflorin attenuates hepatic ischemia/reperfusion injury *via* anti-oxidative, anti-inflammatory and anti-apoptotic pathways. Exp Ther Med 2016; 11: 263-8.
39. Zheng YZ, Bu JM, Yu L, Chen J, Liu HG. Nobiletin improves propofol-induced neuroprotection *via* regulating Akt/mTOR and TLR 4/NF-κB signaling in ischemic brain injury in rats. Biomed Pharmacother 2017; 91: 494-503.
40. Lee KI, Su CC, Fang KM, Wu CC, Wu CT, Chen YW. Ultrafine silicon dioxide nanoparticles cause lung epithelial cells apoptosis *via* oxidative stress-activated PI3K/Akt-mediated mitochondria- and endoplasmic reticulum stress-dependent signaling pathways. Sci Rep 2020; 10: 9928.
41. Peng HB, Wang RX, Deng HJ, et al. Protective effects of oleanolic acid on oxidative stress and the expression of cytokines and collagen by the AKT/NF-κB pathway in silicotic rats. Mol Med Rep 2017; 15: 3121-8.
42. Jiang FS, Li MY, Wang HY, et al. Coelonin, an anti-inflammation active component of bletilla striata and its potential mechanism. Int J Mol Sci 2019; 20: 4422.
43. He X, Chen S, Li C, et al. Trehalose alleviates crystalline silica-induced pulmonary fibrosis *via* activation of the TFEB-mediated autophagy-lysosomal system in alveolar macrophages. Cells 2020; 9: 122.